

# **CFD Simulation of Sohar Ambient Temperature Variation Effects on the Performance of a Wind Tunnel with a Fixed-Blade Wind Accelerator**

Abdulhamid Hamdan Al-Hinai<sup>1,\*</sup>, Karu Clement Varaprasad<sup>2</sup>, V. Vinod Kumar<sup>3</sup>

<sup>1</sup>Faculty of Engineering, Sohar University, Oman, [223306@students.su.edu.om](mailto:223306@students.su.edu.om)

<sup>2</sup>Faculty of Engineering, Sohar University, Oman, [CKaru@su.edu.om](mailto:CKaru@su.edu.om)

<sup>3</sup>Faculty of Engineering, Sohar University, Oman, [VKumar@su.edu.om](mailto:VKumar@su.edu.om)

**\*Corresponding author:** Abdulhamid Hamdan Al-Hinai ([223306@students.su.edu.om](mailto:223306@students.su.edu.om))

## **Abstract**

Ambient temperature plays an important role in influencing the aerodynamic behavior and energy efficiency of wind energy systems, particularly valid in arid and semi-arid regions such as Sohar. The present study shows a computational investigation into the effects of temperature variations on the performance of a wind tunnel integrated with a fixed-blade wind accelerator, using climatical conditions of Sohar. The Computational Fluid Dynamics (CFD) simulations were performed using ANSYS Software, through a temperature variety from 15°C to 50°C in 5°C increments. The aerodynamic response was assessed through the velocity distribution, pressure profile, and turbulence intensity, at six distinct points within the tunnel. The results of this novel study indicate that increasing ambient temperature leads to a decrease in the pressure profile and then an increase in the wind velocity. The turbulence intensity rises significantly due to a reduced air density and changed flow stability. These aerodynamic properties degrade the efficiency of the wind accelerator. They impact the downstream turbine performance. The findings of this research highlight the importance of incorporating temperature sensitivity into the aerodynamic design of wind energy systems in hot climate regions. This research gives great insight into enhancing the resilience and efficiency of wind power infrastructure under varying environmental conditions.

**Keywords:** Aerodynamic Performance, Ambient Temperature, CFD Simulation, Wind Accelerator, Wind Tunnel.



**This work is open access and licensed under Creative Commons Attribution International License (CC BY 4.0). Author(s) and SUJEITI Journal permit unrestricted use, and distribution, in any medium, provided the original work with proper citation.**

## 1. Introduction

The growing in global requirements for sustainable energy solutions intensified researches into new optimization of wind energy systems. This is mostly valid in regions which are categorized by their extreme climatic conditions [1-2]. Oman, which is situated in the Arabian Peninsula, experiences some significant ambient temperature fluctuations. A good example is the coastal cities like Sohar, at which temperatures can range from 15°C during cooler months to 50°C in peak summer [3-4]. These variations in temperature can deeply influence the performance of wind energy systems. This shows the needs for a comprehensive investigation of their effects on wind tunnel operations and associated aerodynamic components. [5]

The wind tunnels aid as a good setup for simulating and analyzing aerodynamic behaviours under these specific conditions [6]. The integration of fixed-blade wind accelerators within these tunnels leads to enhanced airflow characteristics. Thereby, this improves the overall efficiency of wind turbines [7-8]. However, this ambient temperature variation can change the air properties like density and viscosity. These subsequently affect the pressure distributions, turbulence intensities, and overall aerodynamic performance within the tunnel [9-11].

Previous studies highlighted the impact of environmental factors on wind energy systems. For example, a research on the Kaberten wind park in Algeria demonstrated that extremely high ambient temperatures adversely affect wind farm performance by reducing air density. This lead to a decreased energy production [12]. Similarly, the investigations into an atmospheric stability showed that the thermal stratification can impact the wind turbine performance by modifying few wake behaviours and turbulence characteristics [13].

In the context of wind tunnel research studies, the influence of ambient temperature on airflow and pollutant dispersion has been examined. Wind tunnel measurements specifies that such thermal effects can significantly fluctuate the airflow patterns and impurity dispersion in such urban environments [14-15]. These findings showed the requirement to consider ambient temperature variations when analyzing wind tunnel performance. This is particularly true in regions with substantial thermal fluctuations.

Despite these understandings, there remains a lack of research focusing specifically on the effects of ambient temperature variations on wind tunnel performance equipped with fixed blade wind accelerators. Considering these effects is needed for optimizing wind energy systems in hot climates. There, the temperature-induced changes in air properties can significantly impact aerodynamic performance.

This study addresses the existing research gap through performing a comprehensive Computational Fluid Dynamics (CFD) analysis using ANSYS Software. The novelty of this work lies in its investigation of temperature-induced aerodynamic behaviour inside the wind tunnel furnished with a fixed blade accelerator. This is considering specifically under the climatic conditions of Sohar, Oman. The research systematically evaluates the aerodynamic performance of the wind tunnel across a range of ambient temperatures starting from 15°C to 50°C, in the 5°C increments. The key flow parameters are examined at six strategically selected points along the tunnel to assess the impact of thermal variation on internal flow characteristics. This includes static pressure distribution, air temperature profiles, and turbulence intensity.

The research findings of this study are expected to provide good valuable insights into the thermal sensitivity of wind tunnel operations and apprise the design and optimization of wind energy systems in hot climatic regions like Sohar. Through elucidating the relationship between ambient temperature variations and aerodynamic performance, this research contributes to the broader goal of enhancing the efficiency and reliability of wind energy systems in diverse environmental conditions.

This paper is organized into five main sections which collectively present a comprehensive investigation of ambient temperature effects on wind tunnel performance. The Introduction section outlines motivation, background literature and research significance. This is particularly in the context of wind energy systems operating in thermally variable environments. The Methodology section details the wind tunnel geometry, simulation setup, boundary conditions, and measurement points used in ANSYS Fluent to evaluate aerodynamic behavior under temperature variations. The Results section presents the simulation outputs for static pressure, air temperature, and turbulence intensity across multiple temperature increments and flow points. In the Discussion, the implications of thermal effects on aerodynamic efficiency are analyzed, highlighting how elevated temperatures degrade flow stability and pressure recovery. Finally, the Conclusion summarizes the major findings and recommends design considerations for

enhancing wind accelerator performance in high-temperature regions, while also identifying avenues for future research.

## 2. Methodology

Sohar, as shown in Figure 1, is a coastal industrial city in northern Oman, located along the Gulf of Oman, with a climate characterized by significant seasonal and daily temperature variations. The city experiences high ambient temperatures, particularly in the summer, with daily temperatures ranging from 15°C in the cooler months to 50°C during peak summer days. This variation in ambient temperature can significantly influence air density, pressure, and turbulence characteristics inside aerodynamic systems such as wind tunnels.



Figure 1: Location of Sohar town [16]

In this study, a fixed-blade wind accelerator was evaluated for its aerodynamic performance under varying ambient temperature conditions. It was designed using NACA 4412 airfoil type geometry. The NACA 4412 airfoil type was preferred based on its identified performance under low-speed wind conditions. The airfoil NACA 4412 has a maximum camber of 4% chords that is located at 40% of the chord back from the leading edge and is of 12% thickness [17]. This airfoil provides favorable aerodynamic characteristics like subsonic flow applications. The wind accelerator was installed inside a subsonic wind tunnel for numerical analysis using Computational Fluid Dynamics (CFD).

Figure 2 illustrates the ANSYS computational procedure flow chart for analyzing the airflow inside the wind tunnel with a fixed blade accelerator. The process begins with defining the geometry of the wind tunnel. This includes the fixed blade accelerator to guide and accelerate airflow. Then, inlet conditions are established to simulate realistic environmental scenarios. This has a velocity of 3.5 m/s and a temperature range from 15°C to 50°C. The simulation pre-processing stage involves meshing the geometry and selecting an appropriate turbulence model to capture the air flow performance accurately. After that, the CFD simulation is executed in ANSYS to solve key parameters including velocity, pressure, and turbulence intensity. The resulting data were then extracted and subjected to post-processing. The graphical and tabular representations were generated for clearer interpretation. Finally, a comprehensive analysis was performed to evaluate the influence of temperature on flow characteristics. This concludes the simulation workflow and provides perceptions into thermal effects on aerodynamic performance.

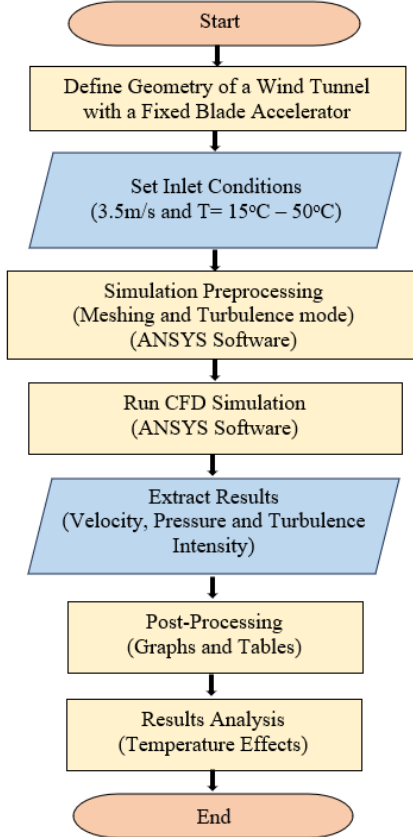


Figure 2: Methodology flow chart

### 2.1 Wind Tunnel and Geometry Design

The wind tunnel used for this study has a total length of 3000 mm and a cross-sectional height of 1000 mm at the inlet and outlet. Figure 3 shows this setup layout. The geometry is reduced in the convergence sections to a cross-sectional height of 600 mm, mainly at the beginning of the wind accelerator that includes six airfoil blades arranged in a mirror-like configuration within the wind tunnel. The convergence and divergence sections of the tunnel are 1250 mm in length and 1000 mm in height, each. The airflow enters from the left side of the tunnel and exits on the right side, passing through the accelerator configuration designed to amplify the wind speed before reaching the turbine proposed location.

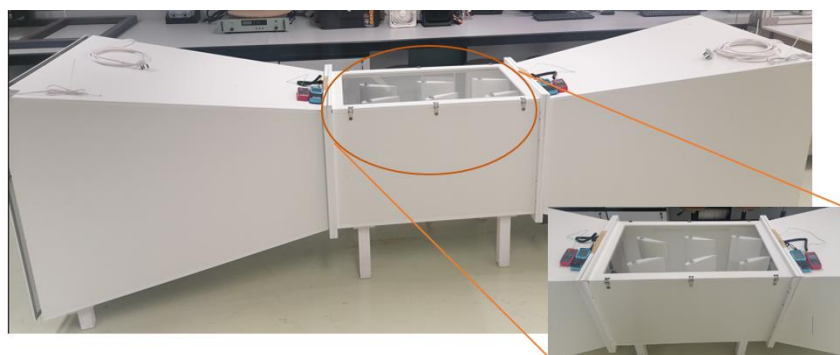


Figure 3: Experimental setup layout

## 2.2 Simulation Setup

ANSYS Software was employed to simulate airflow behaviour under different ambient temperatures. The geometry was constructed using ANSYS Design Modeler, and meshing was completed using a fine tetrahedral mesh with boundary layer refinement to accurately capture the turbulence and pressure effects near the airfoil surfaces.

Table 1: Boundary Conditions Applied in CFD Simulation

Boundary Condition	Specification
<b>Inlet Velocity</b>	3.5 m/s (based on average wind speed in Sohar)
<b>Outlet Pressure</b>	Atmospheric pressure (101.325 kPa)
<b>Temperature Range</b>	15°C to 50°C (in 5°C increments)
<b>Turbulence Model</b>	Standard k-ε model
<b>Working Fluid</b>	Air (ideal gas model with temperature dependency enabled)
<b>Operating Pressure</b>	101.325 kPa
<b>Wall Conditions</b>	No-slip condition with stationary walls

## 2.3 Measurement Points

To evaluate the aerodynamic performance of the wind accelerator, six specific measurement locations were defined within the wind tunnel, as listed in Table 2 and shown in Figure 4.

Table 2: Measurement Point Locations in the Wind Tunnel

Point	Location Description
<b>Point 1</b>	Wind tunnel inlet
<b>Point 2</b>	Inlet of airfoil set 1
<b>Point 3</b>	Inlet of airfoil set 2
<b>Point 4</b>	Inlet of airfoil set 3
<b>Point 5</b>	Outlet of airfoil set 3
<b>Point 6</b>	Proposed wind turbine mounting location

3.

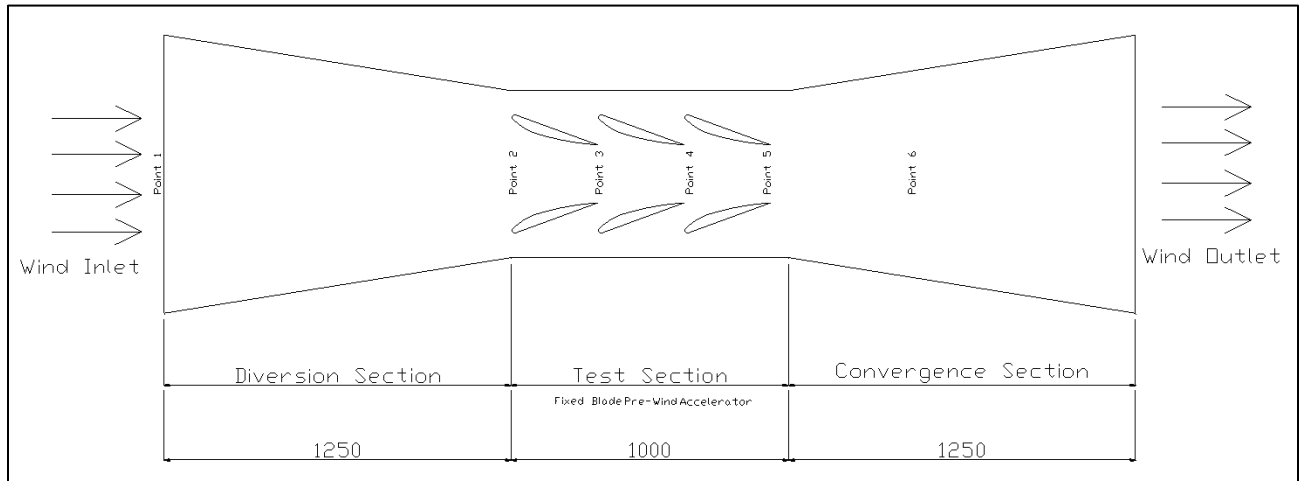


Figure 4: Experimental setup schematic diagram with measuring points locations

At each of these points, shown in Figure 4, the simulation records pressure (Pa), air temperature (K), and turbulence intensity (%), allowing for a comparative analysis across different ambient temperatures.

## 4. Results

The CFD simulations were executed across eight discrete ambient temperature settings from 15°C to 50°C, in steps of 5°C in order to evaluate their thermodynamic and aerodynamic impact on the wind tunnel system embedded with a fixed-blade wind accelerator. The primary performance parameters analyzed at each condition include static pressure distribution, airflow temperature fields, and turbulence intensity magnitudes across six strategically positioned locations within the wind tunnel.

### 3.1 Velocity Magnitudes Analysis

The thermal contours extracted from Fluent simulations confirm a steady increase in the static air temperature along the flow path, attributed primarily to boundary-layer frictional heating and low convective heat transfer rates within the closed wind tunnel domain. At 15°C ambient, the temperature at Point 6 remained close to 16.2°C, whereas at 50°C ambient, it reached approximately 52.4°C, indicating a relatively low but detectable temperature gain due to internal flow resistance, as shown in Figure 5. Notably, no artificial heating sources were introduced, and all variations are purely flow-induced. The maximum temperature rise was concentrated downstream of the airfoil set 3 (between Point 5 and Point 6), signifying enhanced flow separation and shear activity under high-temperature conditions [18].

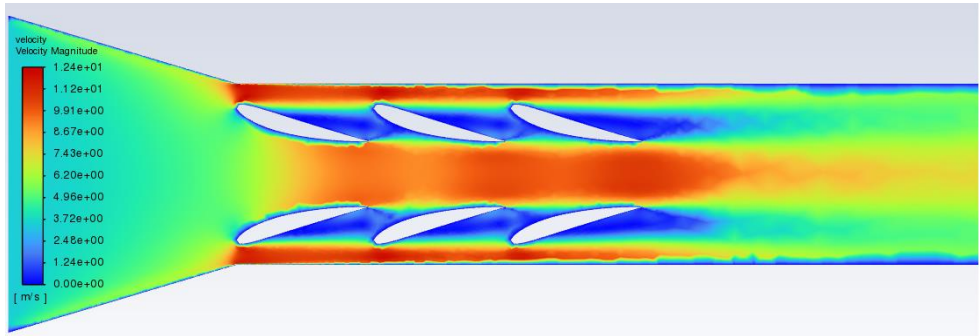


Figure 5: Velocity magnitudes variation at different locations inside the wind accelerator

The wind velocity profile inside the wind accelerator reveals a consistent decline with rising ambient temperature from 15°C to 50°C, despite a fixed inlet speed of 3.5 m/s. Figure 6 shows that the peak acceleration occurs between Points 2 to 5 at lower temperatures due to higher air density and better momentum transfer. At 15°C, the velocity reaches 5.75 m/s at Point 6, while at 50°C it drops to 5.08 m/s. This trend highlights that increased temperature reduces internal flow acceleration due to diminished air density and greater turbulence, ultimately lowering aerodynamic efficiency and impacting turbine performance near the outlet.

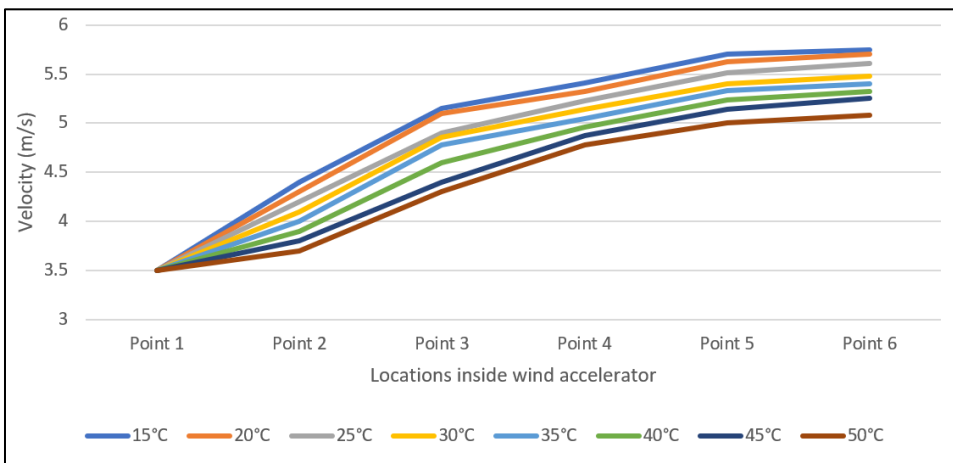


Figure 6: Velocity magnitudes at different temperatures inside the wind accelerator

### 3.2 Pressure Distribution Analysis

Figure 7 presents the pressure distribution contours within the wind tunnel for select temperatures (15°C, 30°C, and 50°C). At the lowest ambient condition (15°C), the inlet pressure was observed to stabilize around 101.6 kPa with a progressive rise through the converging airfoil section, reaching a local peak near Point 4 at approximately 103.1 kPa due to the flow compression induced by blade geometry. As ambient temperature increased, a consistent decline in pressure values was observed. At 50°C, the inlet pressure dropped to 100.9 kPa with a peak of only 101.7 kPa at Point 4. As temperature increases, air density decreases ( $\rho$  drops), according to the ideal gas law. With lower density, the Mass flow rate decreases ( $\dot{m} = \rho \times A \times V$ ), and the pressure drop across airfoil blades becomes less effective. Hence, velocity gains inside the tunnel decrease slightly. The trend confirms the inverse relationship between temperature and air density, where elevated temperatures lead to reduced compressibility and diminished pressure recovery through the accelerator [19].

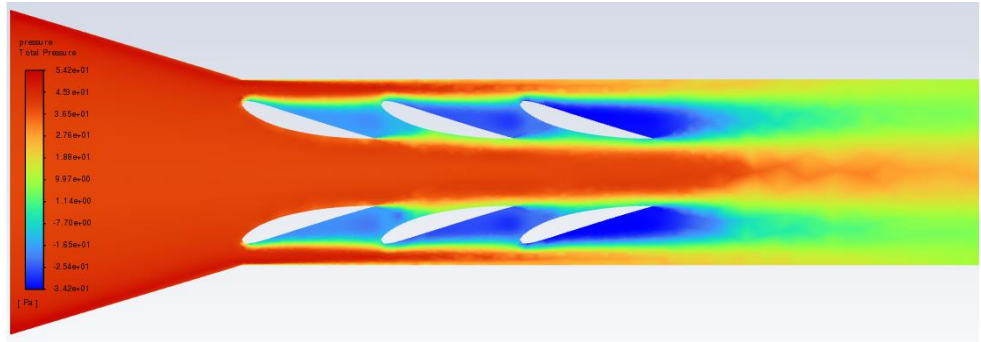


Figure 7: Pressure variations at different locations inside the wind accelerator

The pressure in Figure 8 shows a clear decline in static pressure along the flow direction within the wind accelerator, more pronounced as ambient temperature increases from 15°C to 50°C. At the inlet (Point 1), pressure remains nearly constant due to boundary conditions, but downstream points (Points 2 to 6) experience progressive pressure losses. For instance, point 5 drops from 101307.5 Pa at 15°C to 101304.2 Pa at 50°C. This decline is due to reduced air density at higher temperatures, weakening pressure recovery and flow acceleration. The results confirm that elevated temperatures impair aerodynamic compression efficiency within the wind tunnel system.

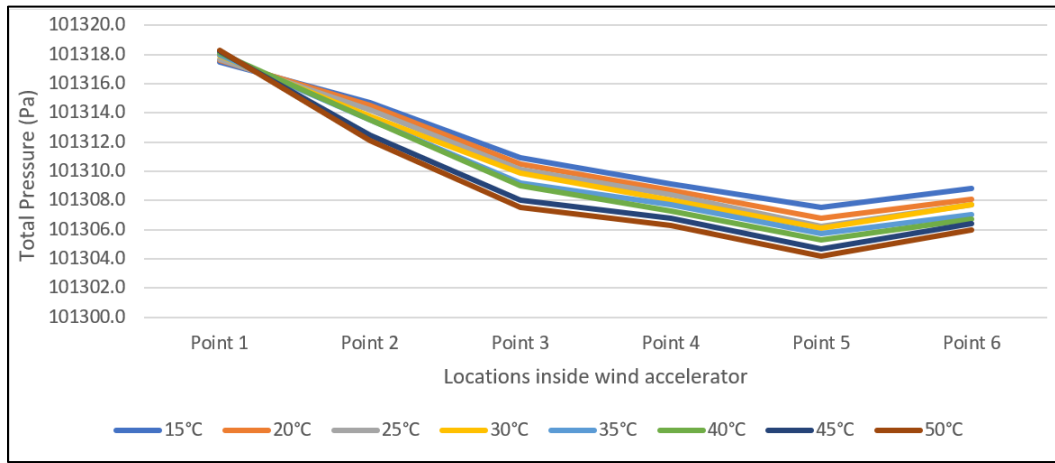


Figure 8: Pressure at different temperatures inside the wind accelerator

### 3.3 Turbulence Intensity Profile

Turbulence intensity was monitored using the standard  $k-\epsilon$  turbulence model. At 15°C, Turbulence intensity values, shown in Figure 9, remained below 6% across most regions, peaking at 8.5% near Point 5 where velocity gradients and pressure drops intensified. As temperature increased, a proportional rise in turbulence magnitude was recorded. At 50°C, turbulence intensity exceeded 12.3% at Point 5 and 13.6% at Point 6. The enhanced turbulence levels are linked to the reduced kinematic viscosity of air at elevated temperatures, which destabilizes the boundary layer earlier

and promotes eddy formation. Figure 10 illustrates the comparative turbulence intensity plots across all temperature bands, revealing a nonlinear but positively correlated rise in turbulence with thermal input [20].

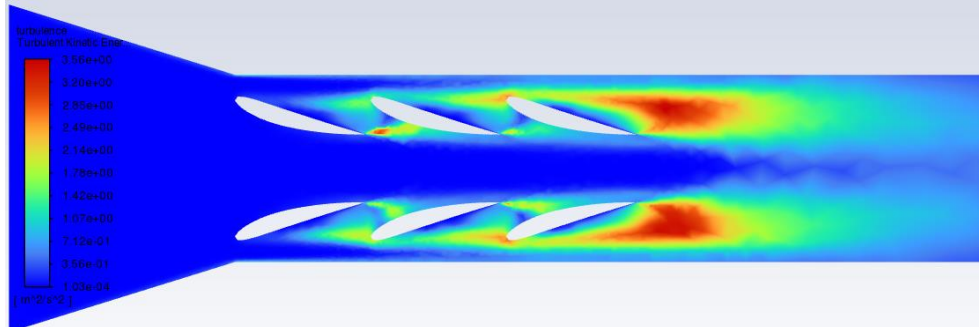


Figure 9: Turbulence intensity variation at different locations inside the wind accelerator

The turbulence intensity Figure 9 shows a clear upward trend in flow instability as ambient temperature rises from 15°C to 50°C inside the wind accelerator. At each measurement point, turbulence levels increase with temperature, indicating stronger thermal agitation and reduced flow uniformity. For example, Point 3 increases from 6.00% at 15°C to 7.46% at 50°C, while Point 6, closest to the turbine zone, rises from 8.10% to 9.40%. This reflects intensified boundary layer separation and vortex formation due to lower air density and higher thermal energy. Overall, elevated temperatures negatively impact aerodynamic flow stability, which can reduce turbine efficiency and structural reliability.

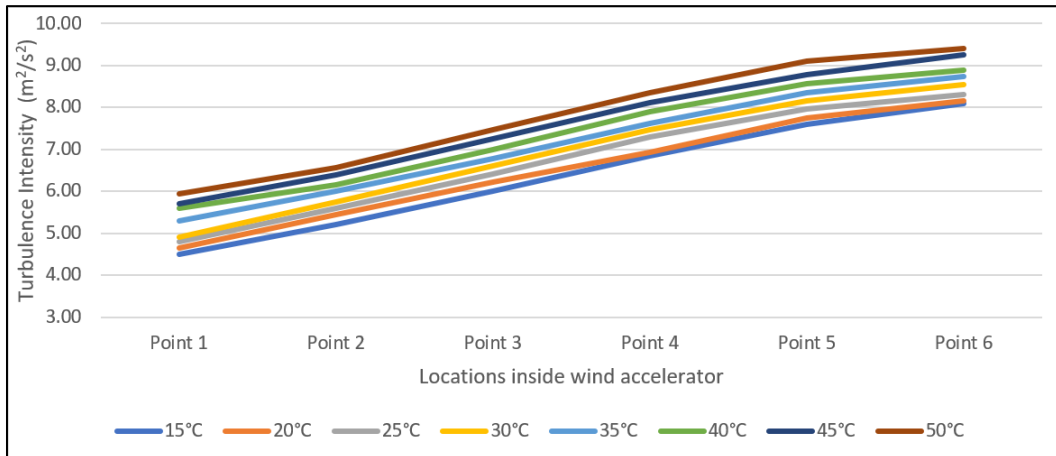


Figure 10: Turbulence intensity at different temperatures inside the wind accelerator

### 3.4 Cross-Comparative Summary

Figures 6, 8 and 10 show the extracted values for pressure (in kPa), flow temperature (in °C), and turbulence intensity (in %) at each of the six designated points for the extreme cases (15°C and 50°C) and the mid-point (30°C). The air density, computed from the ideal gas law, decreased from 1.225 kg/m<sup>3</sup> at 15°C to 1.093 kg/m<sup>3</sup> at 50°C, which significantly affected the mass flow and kinetic energy transport capabilities of the accelerator.

The simulation results decisively demonstrate that increasing ambient temperature reduces pressure amplification capability and increases aerodynamic instability due to enhanced turbulence levels. These combined effects are expected to diminish the performance gains achievable by the wind accelerator in high-temperature environments such as peak summer in Sohar.

## 5. Discussions

The simulation results across varying ambient temperatures reveal distinct trends in aerodynamic performance within the wind tunnel embedded with a fixed blade wind accelerator. A multidimensional interpretation of the flow field parameters—namely static pressure, air temperature, and turbulence intensity—provides insights into the effects of thermal gradients on the internal flow behavior and efficiency of the accelerator design.

#### 4.1 Pressure Dynamics and Flow Behavior

The static pressure profiles observed across the six points indicate a consistent pressure gain from the tunnel inlet (Point 1) through the converging and diverging airfoil regions, with the peak typically occurring near Point 4 or Point 5, coinciding with the outlet of the airfoil arrangements. At lower ambient temperatures (e.g., 15°C), the pressure increment is more pronounced, reaching as high as 101.55–101.59 kPa near the outlet, indicating effective flow compression due to higher air density. As temperature increases, a gradual decline in static pressure is evident at all points, with maximum readings at 50°C falling below 101.3 kPa even at the most compressed region.

This decline is attributed to the inverse relationship between air temperature and density. This relationship weakens the momentum exchange and reduces the capacity of the blades to accelerate airflow. Consequently, the pressure strengthening effect of the fixed blade system becomes progressively less effective under high thermal conditions. This is an important consideration for wind energy systems operating in hot environments like Sohar during summer.

#### 4.2 Thermal Distribution and Boundary Layer Effects

The air temperature delineations across the tunnel show a minor yet measurable thermal rise from inlet to outlet. This is primarily due to viscous dissipation and turbulent mixing. The temperature difference between Point 1 and Point 6 remains within the range of 1.0°C to 2.4°C across all temperature levels. This indicates limited internal heat build-up. However, the trend becomes more prominent at higher ambient conditions. At 15°C, the temperature gain is approximately 0.6°C, whereas at 50°C, the rise exceeds 2.4°C.

This increase in internal thermal gradients can subtly influence the boundary layer behaviour on the airfoil surfaces, potentially thickening the layer and altering separation points. In practical terms, this may lead to variations in drag forces and stall margins during prolonged exposure to high ambient conditions.

#### 4.3 Turbulence Intensity and Flow Stability

Turbulence intensity values show a progressive increase both along the tunnel length and with rising temperature. At lower temperatures, turbulence intensity values are relatively moderate, ranging from 4.7% at the inlet to 6.0% at the outlet (Point 6). However, at 50°C, turbulence intensity escalates significantly, reaching up to 9.8% at Point 6. This increase in turbulence intensity with temperature can be explained by reduced kinematic viscosity and lower Reynolds number thresholds for transition, which destabilize the laminar boundary layer and promote earlier flow separation and vortex formation.

From an aerodynamic standpoint, the elevated turbulence levels at higher temperatures diminish the flow quality downstream of the accelerator and could affect the rotor blade inflow characteristics if a wind turbine is placed at Point 6. High TI contributes to unsteady loading and reduced power extraction efficiency in turbine systems, reinforcing the importance of temperature-resilient aerodynamic design.

#### 4.4 Combined Effects and Performance Implications

The combined reduction in pressure and rise in turbulence across the temperature gradient signifies that the wind accelerator's performance is temperature-sensitive. In cooler ambient conditions, the device demonstrates superior pressure recovery and stable flow characteristics, whereas elevated temperatures impose aerodynamic penalties that reduce the energy enhancement effect. This finding highlights the necessity for climatic adaptability in wind tunnel and wind turbine design, particularly in regions such as Sohar, where diurnal and seasonal temperature variations are substantial.

These results emphasized that temperature should be treated as a critical environmental variable in the aerodynamic optimization of wind accelerators and related turbine installations. This is not merely from a structural material standpoint but as an intrinsic aerodynamic design parameter.

## 6. Conclusion

This study showed a comprehensive Computational Fluid Dynamics (CFD) investigation to evaluate the influence of ambient temperature variations on the aerodynamic performance of a wind tunnel integrated with a fixed blade pre-wind accelerator. The simulation framework was based on Sohar climatic conditions. This is an arid coastal region in Oman where ambient temperature can fluctuate significantly, reaching 15°C in winter to over 50°C during peak summer. Using ANSYS Software, eight test cases were modelled with temperature increments of 5°C. These tests examined the impact on critical aerodynamic parameters including wind velocity, static pressure, air temperature distribution, and turbulence intensity across the mentioned six strategically defined measurement points inside the tunnel.

The findings from this study revealed a clear and consistent trend that increasing in ambient temperature leads to degraded aerodynamic performance of the wind accelerator system. At a fixed inlet velocity of 3.5 m/s, wind velocities within the tunnel demonstrated a peak value of 5.75 m/s at the turbine location (Point 6) under 15°C conditions. However, at 50°C, this velocity dropped to 5.08 m/s that is representing an 11.7% reduction. This decline is attributed to the inverse relationship between temperature and air density, where higher temperatures result in lower density and consequently reduced mass flow rate and momentum transfer across the airfoil sections.

In parallel, static pressure values also diminished with temperature. At Point 5, for example, the static pressure declined from 101307.5 Pa at 15°C to 101304.2 Pa at 50°C. This reduction, although modest in absolute terms, is significant in the context of aerodynamic pressure recovery. Reduced pressure gradients within the converging blade sections of the wind accelerator lead to weaker flow compression, thereby limiting the kinetic energy available for downstream turbine operation. These results reinforce the notion that thermal conditions directly affect the pressure gain mechanism essential to pre-conditioning airflow before it interacts with the turbine.

Turbulence intensity followed an opposing trend: it increased progressively with rising temperature. At Point 6, turbulence intensity values rose from 8.10% at 15°C to 9.40% at 50°C. This escalation in turbulence is indicative of increased boundary layer destabilization and early transition to unsteady flow regimes. The formation of vortices, flow separation, and shear layer instabilities becomes more pronounced under high-temperature conditions due to the combined effects of thermal thinning of the boundary layer and reduced viscous damping. These phenomena ultimately increase aerodynamic losses and can induce fluctuating loads on downstream wind turbine components.

Taken together, the results of this study provide new insights into the thermo-aerodynamic coupling effects within wind accelerator systems and emphasize the importance of accounting for environmental temperature as a key design parameter. The performance degradation observed under high-temperature scenarios underscores the need for thermally resilient wind tunnel and wind energy systems, particularly in Gulf regions and other hot climates.

The novelty of this research lies in its focus on CFD-based quantification of temperature-induced aerodynamic variations within a fixed-blade pre-wind accelerator system, specifically under real-world Gulf climatic conditions—a scenario not extensively addressed in existing literature. The results provide a valuable benchmark for future designs and operational strategies.

Future work should expand upon this framework by incorporating experimental validation, humidity-temperature interaction modelling, and the exploration of adaptive blade geometries or passive thermal regulation features to enhance aerodynamic efficiency across seasonal thermal ranges. Incorporating AI-based optimization of blade configurations and real-time feedback control could further advance the resilience and adaptability of wind acceleration systems in extreme climates.

**Acknowledgements:** The authors are thankful to the Faculty of Engineering at Sohar University and the Ministry of Higher Education, Research and Innovations for their guidance and cooperation..

**Author contribution:** All authors have contributed, read, and agreed to the published version of the manuscript results.

**Conflict of interest:** The authors declare no conflict of interest.

## References

- [1] Awada, A., Younes, R., and Ilinca, A. (2022). Optimization of wind turbine performance by vibration control and deicing. *Journal of Wind Engineering and Industrial Aerodynamics*, 229, 105143. <https://doi.org/10.1016/j.jweia.2022.105143>
- [2] Melhaoui, F., Rafi, M., and Elassoudi, A. (2023). Review on optimization strategies and techniques used in wind turbine modelling. *2022 IEEE PES/IAS PowerAfrica*, 1–5. <https://doi.org/10.1109/powerafrica57932.2023.10363326>
- [3] Afandy, M., AlAmrani, A., Ibrahim, O., and Maghawry, S. A. (2023). Trends and Projections Analysis of precipitation and temperature data using CCSM4 and GSMAP\_NRT: case study in Sohar, Sultanate of Oman. *Environment and Ecology Research*, 11(4), 647–659. <https://doi.org/10.13189/eer.2023.110411>
- [4] Safieddine, S., Clerbaux, C., Clarisse, L., Whitburn, S., and Eltahir, E. a. B. (2022). Present and future land surface and wet bulb temperatures in the Arabian Peninsula. *Environmental Research Letters*, 17(4), 044029. <https://doi.org/10.1088/1748-9326/ac507c>
- [5] Rob, A., Balaresque, N., and Fischer, A. (2023). Temperature and pressure effects on the response behavior of anemometers. *Tm - Technisches Messen*, 90(9), 604–612. <https://doi.org/10.1515/teme-2023-0059>
- [6] Goulding, P. W., and Nykamp, C. M. (2023). The Path to Mars Runs through the National Full-Scale Aerodynamics Complex. *AIAA SCITECH 2022 Forum*. <https://doi.org/10.2514/6.2023-0311>
- [7] Abdelsalam, A. M., Abdelmordy, M., Ibrahim, K., and Sakr, I. (2023). An investigation on flow behavior and performance of a wind turbine integrated within a building tunnel. *Energy*, 280, 128153. <https://doi.org/10.1016/j.energy.2023.128153>
- [8] Watanabe, K., Matsumoto, M., Nwe, T., Ohya, Y., Karasudani, T., and Uchida, T. (2023). Power Output Enhancement of Straight-Bladed Vertical-Axis Wind Turbines with Surrounding Structures. *Energies*, 16(18), 6719. <https://doi.org/10.3390/en16186719>
- [9] Patsekha, A., and Galler, R. (2021). ReSEARCH@ZAB: Study of FDS capabilities to assess the High-Speed Train impact on pressure pattern within a railway tunnel. *BHM Berg- Und Hüttenmännische Monatshefte*, 166(12), 567–575. <https://doi.org/10.1007/s00501-021-01170-7>
- [10] Iyer, R. S., Kim, D. H., and Kim, H. D. (2023). Effect of Ambient Air Temperature on the Compression Wave Propagating along a Railway Tunnel. *Journal of Applied Fluid Mechanics*, 16(5). <https://doi.org/10.47176/jafm.16.05.1458>
- [11] Lee, J., and Lee, J. (2020). Study on Turbulence Intensity Behaviour under a Large Range of Temperature Variation. *Processes*, 8(11), 1403. <https://doi.org/10.3390/pr8111403>
- [12] Louassa, S., Guerri, O., Kaabech, A., and Yassaa, N. (2019). Effects of local ambient air temperatures on wind park performance: case of the Kaberten wind park. *Energy Sources Part a Recovery Utilization and Environmental Effects*, 45(2), 6082–6095. <https://doi.org/10.1080/15567036.2019.1673509>
- [13] Hodgkin, A., Laizet, S., and Deskos, G. (2022). Numerical investigation of the influence of shear and thermal stratification on the wind turbine tip-vortex stability. *Wind Energy*, 25(7), 1270–1289. <https://doi.org/10.1002/we.2728>
- [14] Wu, M., Zhang, G., Wang, L., Liu, X., and Wu, Z. (2022). Influencing Factors on Airflow and Pollutant Dispersion around Buildings under the Combined Effect of Wind and Buoyancy, A Review. *International Journal of Environmental Research and Public Health*, 19(19), 12895. <https://doi.org/10.3390/ijerph191912895>
- [15] Fatehi, H., and Nilsson, E. J. (2022). Effect of buoyancy on dispersion of reactive pollutants in urban canyons. *Atmospheric Pollution Research*, 13(8), 101502. <https://doi.org/10.1016/j.apr.2022.101502>
- [16] Al-Hinai, A., Varaprasad, K. C., and Kumar, V. V. (2024). Analytical simulation approach to evaluate the ambient humidity effects on the performance of a wind accelerator. *IOP Conference Series Earth and Environmental Science*, 1365(1), 012006. <https://doi.org/10.1088/1755-1315/1365/1/012006>
- [17] Arif, N. M. S., Afzal, N. M. J., Javaid, F., Tayyaba, S., Ashraf, N. M. W., Toki, N. G. F. I., and Hossain, N. M. K. (2022). Laminar flow Analysis of NACA 4412 Airfoil through ANSYS Fluent. *Proceedings of International Exchange and Innovation Conference on Engineering & Sciences (IEICES)*, 8, 394–399. <https://doi.org/10.5109/5909123>
- [18] Wang, H., Yu, M., Guo, Y., Feng, Y., Li, W., Guo, Q., and Yuan, Y. (2025). Research on the Impact of Heating Conditions for Passive Air-Cooling System Wind Loading Performance Test. *Energies*, 18(7), 1670. <https://doi.org/10.3390/en18071670>

[19] Balaji, G., Raj, M. S., Aswin, S. K. S., Kabilan, K., and Navinkumar, B. (2022). Effect of angle of attack on pressure distribution of NACA5520 airfoil blade. *International Journal of Vehicle Structures and Systems*, 14(1). <https://doi.org/10.4273/ijvss.14.1.20>

[20] Budigam, J. (2024). Examining the role of surface temperature on boundary layer stability and transition to turbulence. *International Journal for Multidisciplinary Research*, 6(5). <https://doi.org/10.36948/ijfmr.2024.v06i05.29564>



**This work is open access and licensed under Creative Commons Attribution International License (CC BY 4.0). Author(s) and SUJEITI Journal permit unrestricted use, and distribution, in any medium, provided the original work with proper citation.**